Multi-Conductor Flexible Universal Branch Model for Efficient Hybrid AC/DC Power System Load Flow Computation

Lawson, Riley; Sun, Hongbo; Kawano, Shunsuke; Raghunathan, Arvind; Takaguchi, Yusuke

TR2026-114 July 22, 2026

Abstract

The proliferation of inverter based resources (IBRs) in the developing power system has led to a growing interest in the development of hybrid AC and DC systems. These hybrid systems would allow for the simpler integration of these IBRs, many of which operate in the DC domain, with the bulk distribution network. However, the integration of these resources requires techniques to evaluate their impact on system operation, ensuring they operate in a safe and reliable manner. This paper presents a technique to perform load flow analysis on hybrid AC and DC networks which generalizes earlier work on single phase networks. This technique is capable of handling multiphase AC networks, complex system topologies (such as multiterminal or bipolar configurations), diverse inverter control techniques, and component outages, such as the loss of an inverter or transmission line. The scalability and computational efficiency of the method are tested on multiple case studies.

IEEE PES General Meeting 2026

Multi-Conductor Flexible Universal Branch Model for Efficient Hybrid AC/DC Power System Load Flow Computation

Riley Lawson
Dept. of Electrical Engineering
Massachusetts Institute of Technology
Cambridge, MA 02139, USA
lawsonri@mit.edu

Hongbo Sun
Optimization and Intelligent Robotics
Mitsubishi Electric Research Labs
Cambridge, MA 02139, USA
hongbosun@merl.com

Shunsuke Kawano
Advanced Technology R&D Center
Mitsubishi Electric Corporation
Amagasaki, Japan
kawano.shunsuke@dn.mitsubishielectric.co.jp

Arvind Raghunathan
Optimization and Intelligent Robotics
Mitsubishi Electric Research Labs
Cambridge, MA 02139, USA
raghunathan@merl.com

Yusuke Takaguchi
Advanced Technology R&D Center
Mitsubishi Electric Corporation
Amagasaki, Japan
Takaguchi.Yusuke@ce.mitsubishielectric.co.jp

***Abstract*—The proliferation of inverter based resources (IBRs) in the developing power system has led to a growing interest in the development of hybrid AC and DC systems. These hybrid systems would allow for the simpler integration of these IBRs, many of which operate in the DC domain, with the bulk distribution network. However, the integration of these resources requires techniques to evaluate their impact on system operation, ensuring they operate in a safe and reliable manner. This paper presents a technique to perform load flow analysis on hybrid AC and DC networks which generalizes earlier work on single phase networks. This technique is capable of handling multiphase AC networks, complex system topologies (such as multiterminal or bipolar configurations), diverse inverter control techniques, and component outages, such as the loss of an inverter or transmission line. The scalability and computational efficiency of the method are tested on multiple case studies.**

***Index Terms*—hybrid AC/DC networks, inverter based resources, load flow**

I. Introduction

As the power system grows and modernizes, there has been growing interest in developing dedicated DC systems. DC microgrids connected to the bulk AC distribution system pose attractive ways to integrate residential solar and electric vehicles [1]. High voltage DC (HVDC) networks allow for the interconnection of asynchronous AC networks [2], or for feeding isolated loads [3]. The development of these systems, however, poses challenges for system operators to ensure they can operate in safe and reliable manners.

Many different algorithms have been proposed to solve the load flow of a hybrid AC/DC system. Broadly, these algorithms may be categorized in one of three groups: separated, sequential, or unified. Separated algorithms equivalence one of the AC or DC network, and solve the power flow only on the other network. [4] reduces the AC network to a Thévenin equivalent and solves a DC power flow using the AC equivalent network as an input to the system.

Sequential algorithms are those which solve the power flow of each network independently, and communicate information about the interface buses to one another [5]. MatACDC serves as an extension of the AC power flow solver MATPOWER, implementing a separate DC power flow solver on top of MATPOWER [6]. These solvers omit the cross impacts of one system on the other, and require outer loops to drive the two systems to converge at their interfaces within each iteration of the solver leading to solver stability issues on larger systems.

Unified algorithms solve the power flow of the whole network at a time. The authors in [7] present a unified algorithm for single phase networks allowing for unbalanced conditions, however do so by assuming converters inject only positive sequence power, which may not be valid under faulted conditions [8]. The work in [9] uses a multi-conductor model of the DC network to model unbalanced conditions on the DC side, but takes a single phase, balanced approximation of the AC side.

The work in [10] presents a flexible universal branch model to implement a unified hybrid AC/DC power flow solver. This is done by using a branch model capable of modeling all branch components in the network. This unifies both the AC and DC network together. Nodes in the DC network are still treated as having a some voltage angle, however through the implementation of variable capacitance in the model, no reactive power flows into the DC network, keeping the voltage angle constant in the DC network, allowing it to be neglected.

An open area of research is the development of algorithms to handle hybrid multi-phase systems, as previously developed methods have been for single phase networks. This work fills this research gap by generalizing the work of the authors in

[10] to multi-phase networks. This allows for the analysis of complex future power networks, such as multi-terminal DC networks, and to consider the impacts of unbalanced phase conditions or component outages.

The remainder of the paper is organized as follows. Section II details the multi-conductor extension of the flexible universal branch model, including the derivation of the branch admittance matrix representation of the model. Section III derives the mismatch equations to be used in the power flow solver. Section IV details the algorithmic implementation of the unified power flow solver using the previously derived model. Section V presents case studies on large hybrid AC/DC test systems to demonstrate the capabilities of the model. Section VI provides closing remarks.

II. Multi-conductor Model Description

The multi-conductor flexible universal branch model (MC-FUBM) is shown in Fig. 1. This model utilizes three branch models similar to those used in [10]. These branches incorporate multiple sections to represent different technologies. First, they include pi-section models utilized to represent transmission lines, transformer reactances, or output filters of converters. There is also included a variable capacitance which is computed to ensure the net flow of reactive power from AC networks to DC networks is zero. There is an ideal transformer having turns ratio $1 : N_\phi$, where $N_\phi = m_a^\phi e^{j\theta_{sh}^\phi}$, for each phase ϕ, with m_a^ϕ the modulation amplitude and θ_{sh}^ϕ is the shift angle. This transformer is used both to model transformers in the network, as well as to model the action of converters. Finally, the model includes a resistor on the DC port used to model switching losses of the converter. Due to its generality, this model may be used to emulate every branch component in the hybrid AC and DC network.

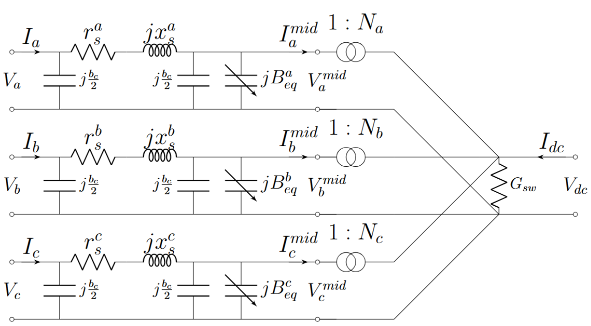

Fig. 1. The multi-conductor flexible universal branch model. Incorporates three FUBM branch models for the AC side of the network, connected to the DC node through a resistor to emulate component losses.

A. MC-FUBM Branch Admittance Matrix

We aim to derive the branch admittance matrix from this branch model, allowing it to be integrated into a power flow problem. First, we define $V^{mid} = [V_a^{mid}, V_b^{mid}, V_c^{mid}]^T$, $V^{ac} = [V_a, V_b, V_c]^T$, $I^{mid} = [I_a^{mid}, I_b^{mid}, I_c^{mid}]^T$, $I^{ac} = [I_a, I_b, I_c]^T$, and $N = [N_a, N_b, N_c]^T$. From inspection of the circuit, we may relate the midpoint voltages at the DC side voltages as

$$V^{mid} = (N^{-1})V_{dc} \tag{1}$$

where the inverse operator here denotes the component wise inverse of the elements of the vector N. For each phase ϕ, the series impedance along the branch is $z_\phi = r_s^\phi + jx_s^\phi$. Define the corresponding admittance $y_\phi = z_\phi^{-1}$. For each phase ϕ, therefore, the inputs and midpoint values are relates as:

$$\begin{bmatrix} I_\phi \\ I_\phi^{mid} \end{bmatrix} = \begin{bmatrix} j\frac{b_c}{2} + y_\phi & -y_\phi \\ -y_\phi & j\frac{b_c}{2} + jB_{eq}^\phi + y_\phi \end{bmatrix} \begin{bmatrix} V_\phi \\ V_\phi^{mid} \end{bmatrix} \tag{2}$$

From (1) and (2), the input current for each phase may be related to the input and DC voltages.

$$I_\phi = \left(j\frac{b_c}{2} + y_\phi\right) V_\phi - y_\phi N_\phi^{-1} V_{dc} \tag{3}$$

The power delivered on the AC side of the circuit is given by the total power delivered from each phase at the mid-point node, $P_{ac} = (V^{mid})^T (I^{mid})^*$. The power delivered on the DC side is given by $P_{dc} = V_{dc} I_{dc}$. The losses in the branch are simulated based on the resistance placed on the DC terminals, and therefore, $P_{loss} = G_{sw} V_{dc}^2$. This allows the power balance equation, $P_{ac} + P_{dc} = P_{loss}$, to be written as:

$$(V^{mid})^T (I^{mid})^* + V_{dc} I_{dc} = G_{sw} V_{dc}^2 \tag{4}$$

Rearranging (4) and substituting in (1) gives:

$$I_{dc} = -(N^{-1})^T (I^{mid})^* + G_{sw} V_{dc} \tag{5}$$

Note that in the DC network, the angle is not used, and therefore $V_{dc}^* = V_{dc}$ and $I_{dc}^* = I_{dc}$. Taking the conjugate of both sides of (5)

$$I_{dc} = -(N^{-1})^{*T} I^{mid} + G_{sw} V_{dc} \tag{6}$$

From (2), we can solve for I^{mid} for any particular phase.

$$I_\phi^{mid} = y_\phi V_\phi - \left(j\frac{b_c}{2} + jB_{eq}^\phi + y_\phi\right)(N^{-1}) V_{dc} \tag{7}$$

Equation (7) can be substituted into (6) to get an expression for the DC current in terms of the AC and DC voltages alone.

$$\begin{aligned} I_{dc} = \sum_{\phi \in \{a,b,c\}} & [(j\frac{b_c}{2} + jB_{eq}^\phi + y_\phi)|N_\phi|^{-2} V_{dc} \\ & - (N_\phi^{-1})^* y_\phi V_\phi] + G_{sw} V_{dc} \end{aligned} \tag{8}$$

Combining (7) and (8) gives the AC and DC currents as functions of the AC and DC voltages, allowing the representation of the MC-FUBM in the conventional admittance matrix representation of a branch component in (9).

Modeling outages of different line components may be done by open circuiting some subset of the branches by setting those phase resistances as $z_\phi = \infty$.

Given this branch model, we can write the nodal power injections. Denote by $S = [S_{dc}, S_a, S_b, S_c]^T$ the vector of complex power injections at each of the DC and AC nodes, respectively, $V = [V_{dc}, V_a, V_b, V_c]^T$, and $I = [I_{dc}, I_a, I_b, I_c]^T$, the extended voltage and current vectors for each port of the

$$\begin{bmatrix} I_{dc} \\ I_a \\ I_b \\ I_c \end{bmatrix} = \begin{bmatrix} \sum_\phi [(j\frac{b_c}{2} + jB_{eq}^\phi + y_\phi)|N_\phi|^{-2}] + G_{sw} & -(N_a^{-1})^* y_a & -(N_b^{-1})^* y_b & -(N_c^{-1})^* y_c \\ -(N_a^{-1}) y_a & j\frac{b_c}{2} + y_a & 0 & 0 \\ -(N_b^{-1}) y_b & 0 & j\frac{b_c}{2} + y_b & 0 \\ -(N_c^{-1}) y_c & 0 & 0 & j\frac{b_c}{2} + y_c \end{bmatrix} \begin{bmatrix} V_{dc} \\ V_a \\ V_b \\ V_c \end{bmatrix} \tag{9}$$

MC-FUBM. Define by Y the matrix on the right hand side of (9). Then:

$$S = V \odot I^* = V \odot (YV)^* \tag{10}$$

where $\odot$ is the element-wise Hadamard product of the two vectors.

B. Unknown Variables in the MC-FUBM

In addition to the conventional unknowns of a power flow problem, being unknown power injections, nodal voltages and angles, the structure of the FUBM model introduces additional unknowns dependent on what each FUBM branch is modeling. For PV and PQ nodes, which will be denoted $\mathcal{I}_{PV}$ and $\mathcal{I}_{PQ}$ respectively, the unknowns are the voltage angle V_a and magnitude V_m.

For converters and phase shifting transformers, the turns ratios of the ideal transformer need to be determined, meaning the m_a^ϕ and θ_{sh}^ϕ need to be solved for. Those configured for active power control is done by controlling the shift angle. This set of branches will be denoted $\mathcal{I}_{sh}$. Those configured for DC voltage and real power droop will be denoted as $\mathcal{I}_{vscIII}$, and is accomplished controlling the shift angle. Those branches configured for AC voltage control or reactive power control will need the modulation amplitude to be determined, and will be referred to as $\mathcal{I}_{Vt}$ and $\mathcal{I}_{Qt}$, respectively.

Additionally, for converters, the variable capacitance, B_{eq}^ϕ needs to be solved for in each phase. This can be done to control either the zero constraint, which insures there is zero net flow of reactive power into the DC network, or for DC voltage control, which will be denoted $\mathcal{I}_{Qz}$ and $\mathcal{I}_{vscII}$, respectively.

This set of unknowns allows us to build an extended set of unknown variables for the network.

$$x = [\mathbf{V_a}, \mathbf{V_m}, \theta_{\mathbf{sh}}, \mathbf{B_{eq}}, \mathbf{m_a}]^{\mathbf{T}} \tag{11}$$

Here, each entry denotes the vector of all unknowns of that kind.

III. Multi-conductor Extended Mismatch Equations

Given some interconnected system, let Y_{bus} be the full interconnected system admittance matrix. To construct this system level admittance matrix, we first must build two system level connection matrices: one for the from side of the models, C_f, and one for the to side of the model, C_t. Here, for converter branches which span AC and DC networks, the from side will denote the DC side of the branch, and the to side will denote the AC side of the branch. Consider some branch i connecting buses j and k. For the multi-conductor model, we consider each phase of each bus as a distinct node. Let bus j be an AC node, each phase may be denoted j_a, j_b, and j_c. in this case, we update the entries of the connection matrices such that

$$C_{t,(i,j_a)} = C_{t,(i,j_b)} = C_{t,(i,j_c)} = C_{f,(i,k)} = 1 \tag{12}$$

Using these matrices, we can build two auxiliary matrices, Y_f and Y_t, which have the property that $Y_f V$ (where V is the vector of nodal voltages) will give the vector of current injections into the from buses, and similarly for $Y_t V$ and the vector of current injections into the to buses.

$$Y_f = \text{diag}(Y_{ff})C_f + \text{diag}(Y_{ft})C_t \tag{13}$$
$$Y_t = \text{diag}(Y_{tf})C_f + \text{diag}(Y_{tt})C_t \tag{14}$$

In equations (13) and (14), Y_{ff} is a vector of the from bus diagonal elements, Y_{tt} is a vector of the to bus diagonal elements, Y_{ft} is a vector of the upper off diagonal terms, and Y_{tf} is a vector of the lower off diagonal terms, each from (9). Once these two matrices have been computed, the full system admittance matrix is found as:

$$Y_{bus} = C_f^T Y_f + C_t^T Y_t + \text{diag}(Y_{shunt}) \tag{15}$$

Using the second form of the equation in (10), the nodal power injections in the interconnected network are

$$S_{bus}(x) = V \odot (Y_{bus} V)^* \tag{16}$$

Letting S_d be the vector of nodal power demands, and S_g the vector of nodal power generation, the nodal power balance equation is:

$$g_{S_b}(x) = S_{bus}(x) + S_d - S_g = 0 \tag{17}$$

From here, we can get the real and reactive power balance equations:

$$g_{P_b}^i(x) = \Re\left(g_{S_b}^i(x)\right) \quad \forall i \in \mathcal{I}_{pq} \cup \mathcal{I}_{pv} \tag{18}$$
$$g_{Q_b}^i(x) = \Im\left(g_{S_b}^i(x)\right) \quad \forall i \in \mathcal{I}_{pq} \tag{19}$$

The power flows can be separated into those into the from and to sides of the branch models:

$$S_f = (C_f V) \odot (Y_f V)^* \tag{20}$$
$$S_t = (C_t V) \odot (Y_t V)^* \tag{21}$$

For those converters which provide real power control, this can be determined by checking the mismatch between the from bus power and the power setpoint, $\hat{P}_f^i$:

$$g_{P_f}^i(x) = \Re(S_f^i(x)) - \hat{P}_f^i \quad \forall i \in \mathcal{I}_{sh} \tag{22}$$

Those converters configured to provide reactive power control, this can be determined by checking the mismatch between the to bus reactive power injection and the reactive power setpoint, $\hat{Q}_f^j$:

$$g_{Q_t}^{j_\phi}(x) = \Im(S_t^{j_\phi}(x)) - \hat{Q}_t^j/3 \quad \forall \phi \in \{a,b,c\}, j \in \mathcal{I}_{Q_t} \quad (23)$$

Here, the setpoint is assumed to be per phase, and as such is divided by three to be per phase.

The zero constraint on the reactive power flow from the AC to DC side of the network was realized by computing the mismatch between the DC side reactive power and zero. However, for the multi-conductor model, we must compute the reactive power flow on each branch. To do so, compute the midpoint power

$$\begin{aligned} S_\phi^{mid} &= V_\phi^{mid}(I_\phi^{mid})^* \\ &= \frac{V_{dc}(-y_\phi V_\phi)^*}{m_a^\phi e^{j\theta_{sh}^\phi}} + \frac{(jb_c/2 + jB_{eq}^\phi + y_\phi)^* V_{dc}^2}{(m_a^\phi)^2} \end{aligned} \quad (24)$$

To satisfy the zero constraint, we write the mismatch equation as:

$$g_{Q_z}^{j_\phi}(x) = \Im(S_\phi^{mid}(x)) - 0 \quad \forall \phi \in \{a,b,c\}, j \in \mathcal{I}_{Q_z} \quad (25)$$

For converters which control the DC side voltage, we may also use the midpoint power to determine the required variable capacitance setting. Given some desired voltage magnitude V_{dc}, the mismatch equation is

$$g_{V_f}^{j_\phi}(x) = \Im(S_\phi^{mid}(x)) \quad \forall \phi \in \{a,b,c\}, j \in \mathcal{I}_{V_{vscII}} \quad (26)$$

For AC side voltage regulation, this is handled by the modulation amplitude of the turns ratio, and is related to the reactive power balance at the AC side node.

$$g_{V_t}^{j_\phi}(x) = \Im(g_{S_b}^{j_\phi}(x)) \quad \forall \phi \in \{a,b,c\}, j \in \mathcal{I}_{V_t} \quad (27)$$

Finally, for those converters which utilize droop control, the droop relates the DC side voltage to the DC side power injection, giving the mismatch equation:

$$g_{P_{dp}}^i(x) = -\Re(S_f^i(x)) + \hat{P}_f^i - k_{dp}(V_{m,f}^i - \hat{V}_{m,f}^i) \forall i \in \mathcal{I}_{vscIII} \quad (28)$$

where $\hat{V}_{m,f}^i$ is the voltage magnitude set point at node i, $\hat{P}_f^i$ is the power set point, and k_{dp} is the converter droop constant.

IV. MC-FUBM Power Flow Implementation

The above described power flow problem was implemented in MATLAB. We begin from a single phase case file prepared for MATPOWER-FUBM [11] and modified it by appending additional buses for each phase in the AC network, and modifying the corresponding set points accordingly. Then, any unbalance or component outage is implemented either by adjusting loading levels, or setting the component active flag to 0 for downed components.

In contrast with conventional power flow calculations, the FUBM model results in an admittance matrix which changes in each iteration. To facilitate faster computation times, we split the computation of the admittance matrix into two different steps. First, those branches which are not converters have their contributions to the admittance matrix computed, as these do not change iteration to iteration. Then, in each iteration, the admittance matrix of only the converter branches is computed. From these two, the system admittance matrix is computed as the sum of the two.

The Newton-Raphson algorithm was applied to solve the system to within a specified error tolerance of ϵ. The initial condition is selected as a system warm start, with unit voltages, phase angles offset by ± 120 degrees, $m_a^\phi = 1$, and $B_{eq} = \theta_{sh}^\phi = 0$ for all nodes. This algorithm is described in general below.

Algorithm 1 MC-FUBM Power Flow

Input: MATPOWER FUBM case file
Output: Power flow solution of the unknown variables x^{k+1}

Convert single phase case file to three phase case
Apply system imbalance or component outage of interest
Compute Y_{bus}^{noconv}
Initialize x^0 with warm start, $k \leftarrow 0$
while $\epsilon < tol$ **do**
  Compute $Y_{bus}^{conv,k}$
  $Y_{bus}^k \leftarrow Y_{bus}^{conv,k} + Y_{bus}^{noconv}$
  Built system Jacobian, J^k
  $x^{k+1} \leftarrow x^k - J^k \setminus f(x^k)$
  $\epsilon \leftarrow \max(||f(x^{k+1})||)$
end while

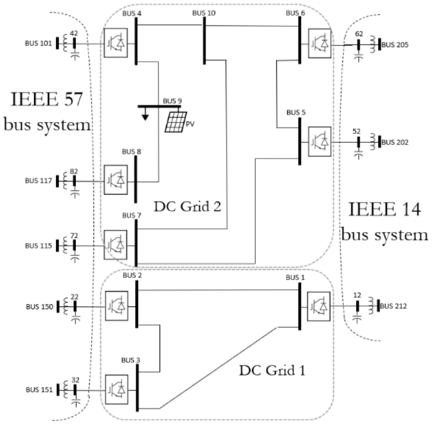

Fig. 2. 81 Bus Test system [12]

V. Case Studies

A. 81 Bus Test Case

The 81 bus test case is formed by interfacing the IEEE 57 and 14 bus test cases through two DC networks, shown in Fig. 2. In each DC network, one converter is configured for DC voltage control, one is configured for zero constraint control, and the remaining feature different control types. This case was considered balanced, as such the voltage magnitude of each phase at each node is identical. The voltage outputs of the power flow are shown in Figs. 3 and 4. The power flow converged in 4 iterations to within a tolerance of $\epsilon = 10^{-12}$, taking a total of 0.3595 seconds.

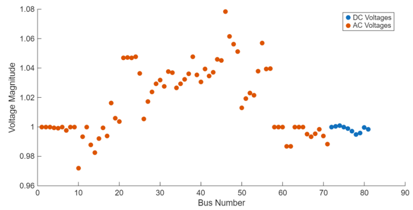

Fig. 3. Voltage magnitude at each node from the power flow for the 81 bus test case

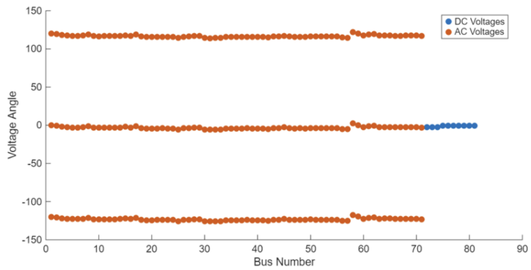

Fig. 4. Voltage angle at each node from the power flow for the 81 bus test case

These results align with the power flow from [12], which converged after 11 iteration in 0.27 seconds within the same tolerance. The increased iteration count may be attributed to an initial condition further from the solution.

B. 324 Bus Test Case

A large test system was created by connecting four copies of the 81 bus test case together. Weak tie lines were added between the AC networks, creating a four area system, each of which is formed from 2 AC networks and 2 DC networks. In this case, unbalance was added by adding a 5% perturbation to the phase A load of every fifth bus in the system. The results of the power flow are shown in Figs. 5 and 6. The unbalanced loading resulted in the depression of some of the phase A voltages. The power flow converged in 4 iterations to within a tolerance of $\epsilon = 10^{-12}$, taking a total of 9.3477 seconds.

VI. Conclusions

This work presented an extended version of the flexible universal branch model capable of handing multiphase systems. This is the first model which can efficiently perform the load flow computation in a multiphase system, while still considering the impacts on both the AC and DC systems without needing to simplify or reduce either system. In this work, these systems are treated as phase-decoupled, as a future extension, the effects of mutual coupling between phases will be included. A computationally efficient algorithm is presented to solve the load flow by splitting the computation of the system admittance matrix into two different steps. The algorithm was then tested on two large test cases, demonstrating its ability to quickly solve these problems.

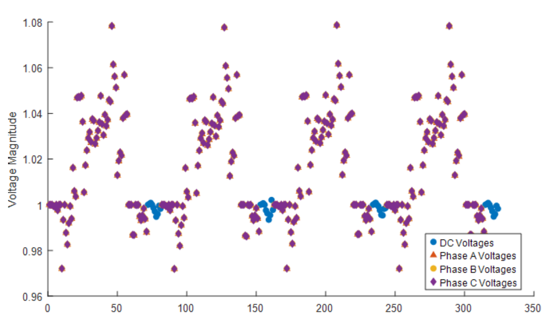

Fig. 5. Voltage magnitude at each node from the power flow for the 324 bus test case

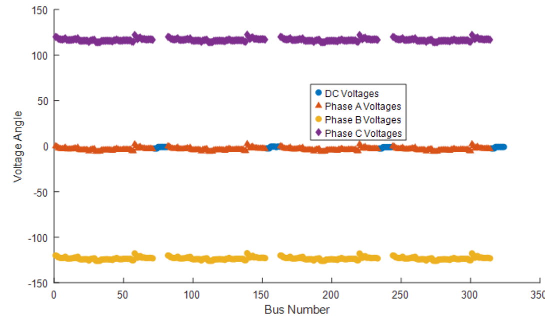

Fig. 6. Voltage angle at each node from the power flow for the 324 bus test case

References

[1] T. Dragičević, X. Lu, J. C. Vasquez, and J. M. Guerrero, "Dc microgrids—part i: A review of control strategies and stabilization techniques," *IEEE Transactions on power electronics*, vol. 31, no. 7, pp. 4876–4891, 2015.

[2] N. R. Watson and J. D. Watson, "An overview of hvdc technology," *Energies*, vol. 13, no. 17, p. 4342, 2020.

[3] N. Flourentzou, V. G. Agelidis, and G. D. Demetriades, "Vsc-based hvdc power transmission systems: An overview," *IEEE Transactions on power electronics*, vol. 24, no. 3, pp. 592–602, 2009.

[4] Z. Li, Y. He, T.-Q. Zhang, and X.-P. Zhang, "Universal power flow algorithm for bipolar multi-terminal vsc-hvdc," *Energies*, vol. 13, no. 5, p. 1053, 2020.

[5] W. Wang and M. Barnes, "Power flow algorithms for multi-terminal vsc-hvdc with droop control," *IEEE Transactions on Power Systems*, vol. 29, no. 4, pp. 1721–1730, 2014.

[6] J. Beerten and R. Belmans, "Matacdc-an open source software tool for steady-state analysis and operation of hvdc grids," in *11th IET International Conference on AC and DC Power Transmission*, p. 088, IET, 2015.

[7] W. Lambrichts and M. Paolone, "General and unified model of the power flow problem in multiterminal ac/dc networks," *IEEE Transactions on Power Systems*, vol. 39, no. 6, pp. 7266–7276, 2024.

[8] J. Zhang, H. Chen, W. Pan, and C. Wang, "Vsc-hvdc control under unbalanced supply conditions," in *2007 IEEE Power Engineering Society General Meeting*, pp. 1–6, IEEE, 2007.

[9] C. K. Jat, J. Dave, D. Van Hertem, and H. Ergun, "Hybrid ac/dc opf model for unbalanced operation of bipolar hvdc grids," *IEEE Transactions on Power Systems*, vol. 39, no. 3, pp. 4987–4997, 2023.

[10] A. Alvarez-Bustos, B. Kazemtabrizi, M. Shahbazi, and E. Acha-Daza, "Universal branch model for the solution of optimal power flows in hybrid ac/dc grids," *International Journal of Electrical Power & Energy Systems*, vol. 126, p. 106543, 2021.

[11] A. Alvarez-Bustos, "MATPOWER-FUBM." https://github.com/AbrahamAlvarezB/matpower-fubm, 2020. Accessed: 2025-10-18.

[12] A. Alvarez-Bustos, *Flexible universal branch model for steady state operational analysis and optimisation of hybrid AC/DC grids*. PhD thesis, Durham University, 2021.